Nanoscale

PAPER

View Article Online
View Journal | View Issue

Cite this: *Nanoscale*, 2014, **6**, 4652

Photo-redox activated drug delivery systems operating under two photon excitation in the near-IR†

Tania M. Guardado-Alvarez,[a] Lekshmi Sudha Devi,[a] Jean-Marie Vabre,[b] Travis A. Pecorelli,[a] Benjamin J. Schwartz,[a] Jean-Olivier Durand,[c] Olivier Mongin,[bd] Mireille Blanchard-Desce[be] and Jeffrey I. Zink*[a]

Received 19th November 2013
Accepted 17th February 2014

DOI: 10.1039/c3nr06155h

www.rsc.org/nanoscale

We report the design and synthesis of a nano-container consisting of mesoporous silica nanoparticles with the pore openings covered by "snap-top" caps that are opened by near-IR light. A photo transducer molecule that is a reducing agent in an excited electronic state is covalently attached to the system. Near IR two-photon excitation causes inter-molecular electron transfer that reduces a disulfide bond holding the cap in place, thus allowing the cargo molecules to escape. We describe the operation of the "snap-top" release mechanism by both one- and two-photon activation. This system presents a proof of concept of a near-IR photoredox-induced nanoparticle delivery system that may lead to a new type of photodynamic drug release therapy.

Introduction

Photodynamic therapy is an established method for treating several medical indications such as lung[1] and oesophageal[2] cancer. Although the most common form of phototherapy uses nontoxic compounds that become toxic upon light irradiation (*e.g.* singlet oxygen formation from an FDA-approved porphyrin containing drug),[3] there is a need for more general treatment methods, especially delivery of apoptosis-inducing anticancer drugs. In particular, we wish to take advantage of light activated release of desired intact cargo molecule because it offers the advantages of both temporal and spatial control[4–13] over cargo delivery. A platform that is under active investigation for drug delivery is mesoporous silica nanoparticles (MSNs). Silica provides ease of functionalization, a robust support and little to no biotoxicity[12,14–24] Several methods have been used in order to give the silica nanoparticles different material qualities that render them useful for drug delivery. One such method is surface modification, which is done by taking advantage of the chemistry of the surface silanol groups.[17,19,20,24–30] This chemistry is used to attach molecular machines to the nanoparticle surface, allowing the particles to act as delivery system that can be activated upon command. Several examples of photodynamic activation of delivery systems in MSNs have been reported, including a supramolecular system that involves a cyclodextrin threaded onto an azobenzene-based molecule grafted onto the surface of MSNs that functions as a nanocarrier and is activated using ultraviolet (UV) light.[12] Multiple examples of azobenzene derivatives that are attached to the interiors of pores, are static in the dark and hold cargo molecules in the pores but act as impellers when irradiated and release the cargo are also known.[31,32] Another variation involves direct photocleavage of a bulky group blocking the pore openings, leading to the release of cargo.[10,25]

A major drawback of the photo-activated systems mentioned above is the need for a high energy (frequently UV) light source to break a chemical bond to initiate delivery; such light has limited tissue penetration and thus these systems have limited applicability for internal drug delivery. The optimal wavelengths for tissue penetration are within the biological spectral window (typically 800–1100 nm)[33–35] but the excited states of common photo-activatable groups do not classically absorb at these wavelengths. One way of using near-IR wavelengths for activating systems that require higher-energy photons is *via* simultaneous two-photon excitation (TPE). The two-photon excitation process is nonlinear process, whose probability depends on the square of the intensity of the light (thus leading to intrinsic 3D resolution when using focused light), and involves selection rules different from those for one-photon absorption.[36,37] Two-photon activation can be highly advantageous in biological

[a]*Department of Chemistry and Biochemistry and California NanoSystems Institute, University of California, Los Angeles, California 90095-1569, USA*

[b]*Chimie et Photonique Moléculaires, CNRS UMR 6510, Université de Rennes 1, Campus de Beaulieu, F-35042 Rennes Cedex, France*

[c]*Institut Charles Gerhardt Montpellier, UMR 5253 CNRS-UM2-ENSCM-UM1, CC1701 Place Eugène Bataillon, 34095 Montpellier Cedex 05, France. E-mail: jean-olivier.durand@um2.fr*

[d]*Institut des Sciences Chimiques de Rennes, CNRS UMR 6226, Université de Rennes 1, Campus de Beaulieu, 35042 Rennes Cedex, France*

[e]*Univ. Bordeaux, Institut des Sciences Moléculaires, CNRS UMR 5255, 351 Cours de la Libération, F-33405 Talence Cedex, France*

† Electronic supplementary information (ESI) available: ssNMR, UV-vis spectra of 2PNT, pXRD, synthesis of 2PNT. See DOI: 10.1039/c3nr06155h

systems[35] as it allows deeper tissue penetration (due to reduced scattering of NIR light) and addresses more spatially selected zones as the TPE processes allows intrinsic excitation confinement to the focal regions where the excitation intensity is the highest. Side photodamages can also be reduced depending on excitation intensity required to achieve TPE in the NIR range. This is particularly the case when chromophores having much larger TPE response (typically orders of magnitude larger) than endogenous chromophores are designed.[38] As endogenous chromophores have two-photon absorption cross-sections in the biological spectral window not larger than a few GM (for the more effective ones, *e.g.* flavins),[39] efficient TPE for bioapplications requires chromophores having TPA cross-sections typically larger than 100 GM. An appealing concomitant benefit of TPE for bioapplications is provided by the larger dynamic range in two-photon as compared to standard one-photon excitation cross-sections allowing more selective excitation (or higher contrast) *via* two-photon excitation in the NIR than standard one-photon excitation in the UV-vis region.[36,37]

Unfortunately the two-photon absorption cross-sections in the NIR region of most effective light-responsive delivery systems are too small and do not meet the above criteria. A way to circumvent this inherent difficulty while taking advantage of efficacy of common light delivery systems is to couple efficient two-photon absorbers with efficient (one-photon) activatable delivery systems. Such strategy has been successfully applied for efficient neurotransmitter photorelease under two-photon excitation in the NIR range (based on coupling *via* FRET mechanism).[40] By combining suitable two-photon-absorbing transducers with nanomachines on MSNs, many existing drug delivery therapeutic systems could be modified to function under TPE using tissue penetrating near-IR light.

In this paper, we present a proof-of-concept nanomachine system stimulated by chemical reduction that has been reconfigured for two-photon light activation (Fig. 1). The system takes advantage of the two-photon activated photo-transducer N^1-(4-((1*E*,3*E*)-4-(4-(dipropylamino)phenyl)buta-1,3-dien-1-yl)phenyl)-N^1-propylethane-1,2-diamine (2PNT), whose chemical structure is shown in Fig. 1, to reduce a disulfide bond and release cargo from MSNs. Direct photolysis of similar disulfide-based systems has been investigated previously, but the photolysis typically requires short wavelength light sources.[17] To the best of our knowledge, photocleavage of a disulfide bond has not been used for drug delivery purposes, and this work constitutes the first example of the use of NIR photo-induced disulfide bond breaking to release cargo from MSNs carriers.

Prior work on a molecule similar to 2PNT has shown that electrons are generated through a reversible photo-oxidation of the neutral molecule to the dication.[41] This is because the 2PNT molecule is a conjugated donor–π–donor system (typically leading to significant TPA cross-sections) bearing electronegative end groups. Upon excitation it becomes a photo-reducing agent that operates at low oxidation potentials.[41,42] Thus, when photo-excited, the 2PNT transducers will transfer electrons to the delivery system (snap-top), cleaving the disulfide bond, which in turn uncaps the pore and allows the cargo to be released as shown in Fig. 1. For our system, we use a disulfide

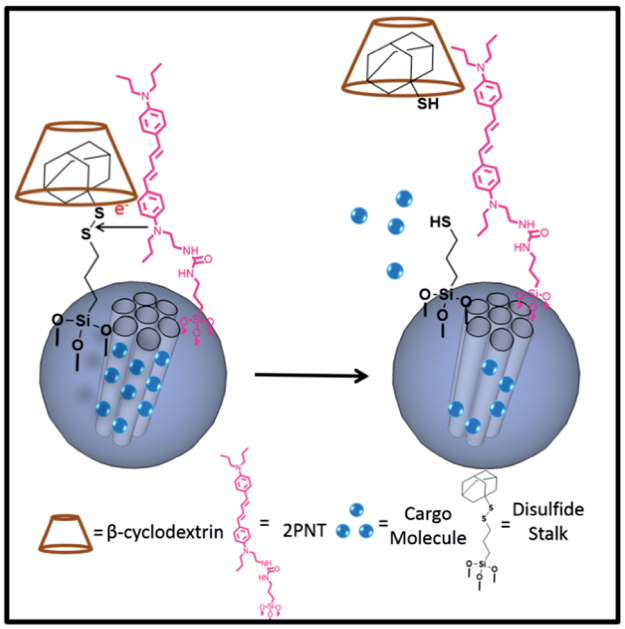

Fig. 1 Disulfide snap-top opening mechanism. Photo-excitation of the photosensitizer causes an electron transfer to the snap-top cleaving the disulfide bond and opening the nanopores.

based snap-top (3-(adamantan-1-yldisulfanyl)propyl)triethoxysilane associated to β-cyclodextrin (due to hydrophobicity) to act as a gatekeeper for the nanopores. To use the 2PNT on the surface of MSNs for transferring an electron to the disulfide bond, it is necessary to inhibit back electron transfer, and therefore we also use a sacrificial agent (EDTA) that donates an electron to the oxidized 2PNT. The combination of the 2PNT transducer, sacrificial EDTA electron donor and releasable snap-top allows our system to be activated on command *via* either one UV photon or two near-IR photons. The activation can release a wide variety of cargo molecules, and the photo-transducer is generalizable to a wide variety of reduction processes.

Experimental

Attachment of the disulfide snap-top to MSN surface

The MCM-41 nanoparticles were synthesized using a base-catalyzed sol–gel procedure previously described in the literature.[8,16,17,43–45] In a round bottom flask, the 2PNT (5×10^{-5} mol, 20.3 mg) was dissolved in 2 mL of ethanol. After the 2PNT was completely dissolved, 3-isocyanatopropyltriethoxysilane (5×10^{-5} mol, 12.4 μL) was added to the flask and left stirring overnight at room temperature under an inert nitrogen atmosphere. In a separate round bottom flask, 10 mL of dry toluene were mixed with 100 mg of surfactant-extracted MSNs. The solution was added to the nanoparticle solution so the 2PNT would condense on the particles' surfaces. The nanoparticle–2PNT mix was heated to reflux and stirred overnight under an inert nitrogen atmosphere. The next day the particles were washed with methanol and water to afford 2PNT-linked mesoporous silica nanoparticles (2PNT-linked MSNs).

The disulfide snap-top was attached to the surface of the 2PNT-linked MSNs. In a round bottom flask 100 mg on the 2PNT-linked MSNs were dissolved in 15 mL of dry toluene and 3-(triethoxysilyl)-1-propanethiol (5×10^{-5} mol, 12.1 μL) and the mixture was heated to reflux and stirred overnight under an inert nitrogen atmosphere. The next day the product was washed with methanol and toluene to remove any excess 3-(triethoxysilyl)-1-propanethiol adsorbed on the surface. Separately in a container lead(II) thiocyanate was combined with bromine in 10 mL of chloroform to yield lead(II) bromide and thiocyanogen. 1-Adamantanethiol (5×10^{-5} mol, 0.0085 mg) was added to this toluene mixture. The thiocyanogen was removed from the reaction as a yellow liquid and slowly added to the 2PNT-linked MSNs toluene solution while the reaction was stirred at 4 °C under a nitrogen atmosphere for four days. The product was then washed thoroughly to remove molecules adsorbed on the surface of the MSNs. After the disulfide snap-top was fully assembled on the surface of the MSNs, the particles were soaked in a concentrated dye solution for 24 h to allow the dye molecules to diffuse into the pores of the MSNs. Then β-cyclodextrin was added and the solution stirred for an additional 24 h to allow β-cyclodextrin to associate with the adamantane molecule due to hydrophobicity. The bulky β-cyclodextrin acts as a pore cap preventing the cargo from escaping (ESI†). After β-cyclodextrin is associated to the adamantane the MSNs were washed thoroughly to remove any dye that was adsorbed on the surface.

Characterization of the disulfide snap-top functionalized MSNs

The pore structure of MCM-41 nanoparticles was confirmed using powder X-ray diffraction (PXRD) and transmission electron microscopy (TEM). From the TEM images the pore diameter was calculated to be about 2.5 nm and the particle size about 100 nm (Fig. 2a). From the PXRD the higher order peaks observed can be indexed as the (1 0 0), (1 1 0) and (2 0 0) planes with a lattice spacing of 4 nm (Fig. 2b). The N_2 absorption–desorption isotherms showed a specific surface area of 1044 m^2 g^{-1}. A ^{13}C ssNMR was taken of the 2PNT–MSNs showing peaks in the aromatic region corresponding to the 2PNT molecule. Furthermore, the ^{29}Si ssNMR of the sample confirmed the functionalization of the silica showing peaks at ~60 ppm corresponding to the silica functionalization and at ~100 ppm corresponding to the silica framework (ESI†).

The attachment of the 2PNT was also confirmed using excitation emission spectra showing peaks at around 350 nm for the excitation and around 480 nm for the emission spectra which match the emission-excitation peaks of the 2PNT in solution (Fig. 2c). The emission spectra of the capped and Rhodamine B loaded nanoparticles was taken showing an emission peak at around 580 nm (Fig. 2d).

General methods for fluorescence spectroscopy

The photo-continuous fluorescence spectroscopy was done using a monochromator connected to an Acton SpectraPro 2300i CCD and excitation by a coherent cube laser. A femtosecond Ti:Sapphire amplifier (Coherent, Legend Elite) seeded with a broadband Ti:Sapphire oscillator (Coherent, Mantis) was used for the two photon excitation. The amplifier output consisting of 40 fs, 60 μJ pulses centered on 800 nm (at 1 kHz repetition rate) was focused to a 2.5 mm spot size.

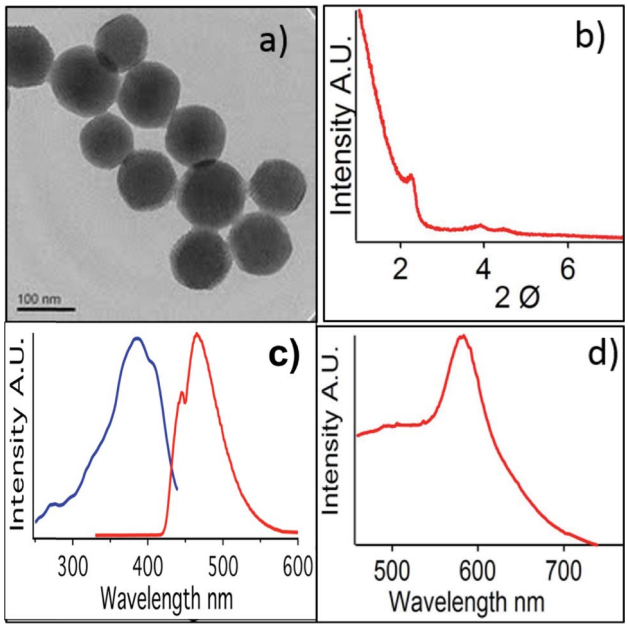

Fig. 2 (a) Transmission electron microscope image of surfactant extracted MCM-41 silica nanoparticles showing the hexagonal pore structure. (b) Powder XRD of the surfactant extracted MCM-41 silica nanoparticles. (c) Excitation spectrum of the 2PNT–MSNs (left) and emission spectrum of the 2PNT–MSNs (right). (d) Emission of the Rhodamine B loaded and capped nanoparticles.

Results and discussion

The operation of the snap-top was monitored by measuring the cargo released from the particles into the solution using continuous monitoring by fluorescence spectroscopy. The dye-loaded snap top-2PNT-linked MSNs were placed in one corner of a two-by-one centimeter glass cuvette (ESI†). Distilled water (pH ~ 7) was carefully added to the cuvette in order to prevent the particles from mixing into the solution. In the opposite corner of the cuvette, a stirring magnet was placed to gently mix the released dye into the solution. The cuvette was then placed in front of the monochromator to measure the fluorescence intensity (ESI†).

Chemical snap-top operation

The activation of the snap-top container is based on the cleavage of disulfide bonds when they are reduced.[46,47] Mercaptoethanol causes chemical cleavage by the mechanism shown in Scheme 1.[17,48–50] The reagent needs to be added in excess to drive the reaction equilibrium to the desired side. The modified particles loaded with pinacyanol iodide cargo were placed in front of a monochromator and the release of the dye monitored using 448 nm excitation. A baseline was taken for 80

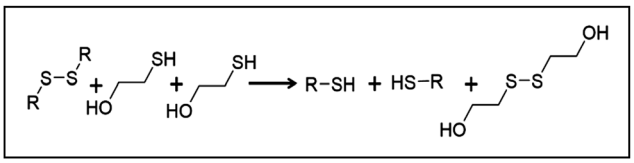

Scheme 1 Disulfide chemical reduction mechanism.

minutes to check for any unwanted leakage of the dye. No increase in fluorescence intensity was observed during this time proving that the snap-top system successfully contains the cargo without any premature leakage. Then 2-mercaptoethanol was added in order to chemically reduce the disulfide bond. The cleavage of the disulfide bond releases the cap, unblocks the pores and allows the cargo to escape in to solution. As a result, the fluorescence intensity immediately increases as shown in Fig. 3a. This experiment confirmed that the system is functional upon the attachment of the 2PNT on the surface of the nanoparticles.

One-photon stimulated release experiments

The snap-top system was then tested for light activation. In this process, photo-excited 2PNT transfers an electron to the disulfide bond, causing cleavage of the disulfide bond. For this experiment, the pinacyanol iodide-loaded particles were set up in a similar fashion as previously described for the chemical reduction. Ethylenediaminetetraacetic acid (EDTA) was added to the aqueous solution as a sacrificial agent that donates an electron back into the 2PNT and reduces back electron transfer. A baseline was taken for 95 minutes to verify that there was no unwanted leakage of the dye. Then the 408 nm pump laser was directed into the particles precipitate and was turned on. The laser excited the 2PNT and induced electron transfer to the disulfide bond. The disulfide bond was cleaved, which removed the cap from the nanopores and allowed the cargo to escape into solution. The release profile was measured by the increase in fluorescence intensity, which plateaued after 8 hours, indicating that the release was complete (Fig. 3b).

A control experiment was carried out to study the system in the absence of a sacrificial electron donating agent. To verify that the system is in fact activated by an electron transfer from the nanotrigger to the disulfide bond, we removed the EDTA to increase the rate of back electron transfer and decrease/stop the activation of the system. A baseline was taken for 140 minutes with no premature leakage of the dye, after which the 408 nm pump laser was turned on (Fig. 3c). No increase in fluorescence intensity of the dye was observed, showing that no cargo escaped because the disulfide bond was not cleaved. After 150 minutes, EDTA was added to the cuvette resulting in an increase in the fluorescence intensity. This experiment shows that the disulfide bond is cleaved only after the 2PNT is able to transfer an electron to the disulfide bond and the back electron transfer is suppressed. It is important to note that this experiment also shows that electron transfer but not thermal heating is the major factor in the activation of the system, since the presence

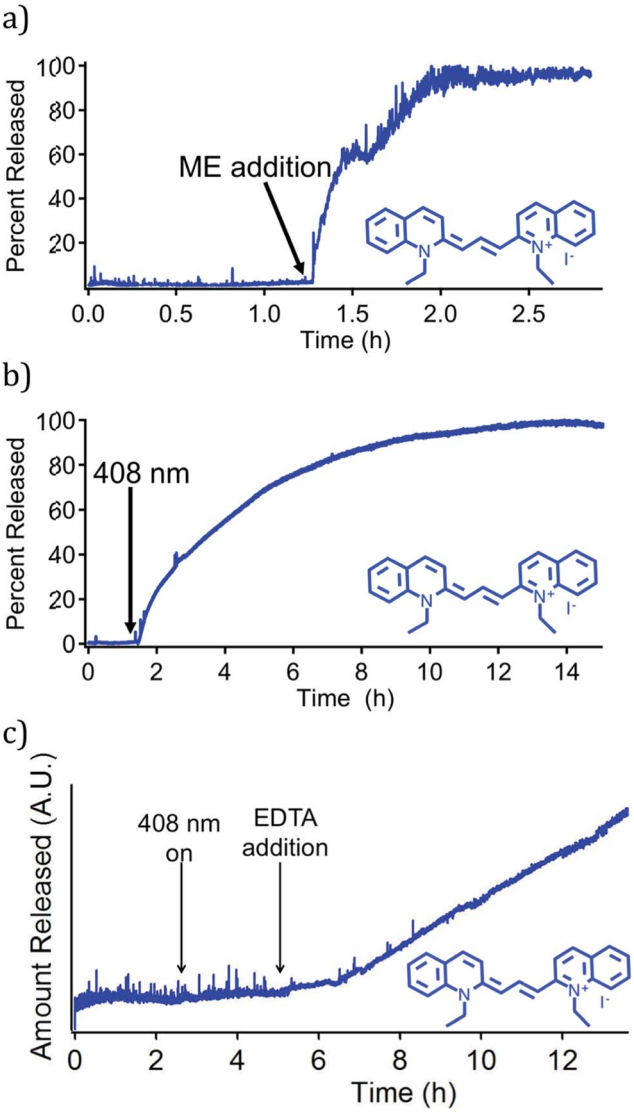

Fig. 3 (a) Release profile of pinacyanol iodide dye from the nanopores by chemical reduction of the disulfide snap top. The arrow points to the addition of mercapto ethanol to the solution after 75 minutes. (b) Release profile of pinacyanol iodide (EDTA was added to the solution) by the light induced electron transfer from the 2PNT when excited by a 408 nm laser source. The arrow points to the activation of the 408 nm pump laser. EDTA acts as a sacrificial agent that donates an electron to the 2PNT reducing back electron transfer. (c) Release profile of pinacyanol iodide in a solution without EDTA. The first arrow indicates when the 408 nm pump laser was turned on and no increase in fluorescence is observed. The second arrow points to the addition of EDTA and the fluorescence of the dye starts increasing. This proves that the opening of the snap top only occurs when the sacrificial agent is present and the back electron transfer to the 2PNT is minimized.

of transparent EDTA cannot change the amount of heat generated by absorption of the laser light.

Two-photon stimulated release experiments

To investigate the activation of the snap-top by two-photon excitation of the sensitizer, we used an ultrafast laser that emits 800 nm light as the excitation source. Since the UV-Vis absorption

spectrum of the sensitizer shows no absorption at 800 nm (ESI†), a two-(or more) photon process is required for photo-activation. The 2PNT chromophore has a TPA cross-section larger than 100 GM at 800 nm, allowing efficient TPE under fs laser excitation at 800 nm.[36,37] The laser system used for the two-photon activation studies was not located near the *in situ* continuous fluorescence monitoring set-up we used in the case of chemical and one-photon activation, so we had to slightly modify the way we performed the release measurements for the two-photon case. The cuvette was set up in a similar manner to the one-photon experiment, and the sample was irradiated with 800 nm fs light pulses for a fixed interval of time (60 minutes). Aliquots of the supernatant that contained the released cargo were taken after each interval and the fluorescence intensity was measured externally. After the measurements, the aliquots were returned carefully to the cuvette prior to subsequent irradiation. The release profiles for two-photon activation of the functionalized and loaded MSNs were measured using Rhodamine B instead of pinacyanol iodide as the cargo due to its photostability and high fluorescence quantum yield. As in the one-photon experiments, EDTA was added to the aqueous solution in the cuvette to act as a sacrificial electron donating agent. The fluorescence intensity of several aliquots were measured prior to the 800 nm irradiation to verify the absence of premature cargo leakage (the flat baseline indicates no increase of fluorescence intensity over time). After the baseline was established for 135 minutes, the 800 nm femtosecond pulsed laser was turned on. An immediate increase of the fluorescence intensity of the dye was observed. Aliquots were taken out for fluorescence measurement every sixty minutes for a total of four hours. During this time, the fluorescence intensity consistently continued to increase indicating that the dye is released in to the solution. The release profile shown in Fig. 4a verifies that two-photon excitation of the sensitizer followed by electron transfer to the disulfide bond cleaves the bond holding the cap in place and allows the cargo to escape.

The femtosecond pulsed laser used for this study can produce high peak powers that might possibly be able to break the disulfide bond directly by two-photon photodissociation. Thus, in order to prove that the system was activated by electron transfer and that direct two-photon induced disulfide bond break was not occurring in operating conditions, we ran control experiments where no EDTA was added to the solution. A baseline was established once more to verify that there was no unwanted dye leakage. Excitation by the femtosecond pulsed laser was initiated after 180 minutes. As expected in the absence of EDTA, the back electron transfer was not suppressed and the disulfide bond was not cleaved. Thus, this experiment confirms the two-photon electron transfer mechanism of activation (Fig. 4b).

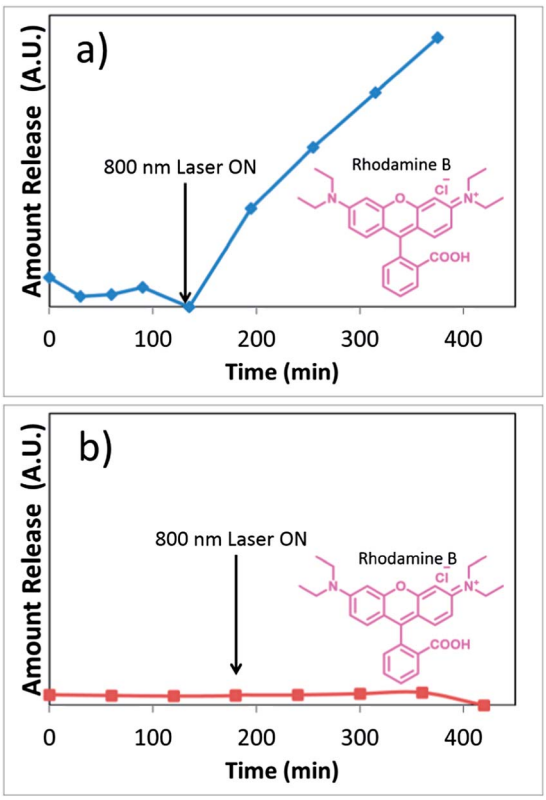

Fig. 4 (a) Release profile of rhodamine B before and after the 800 nm pump laser has been turned on (shown by the arrow) with EDTA present in the aqueous solution. EDTA acts as a sacrificial agent that donates an electron to the 2PNT reducing back electron transfer. (b) Release profile of rhodamine B before and after the 800 nm pump laser has been turned on (shown by the arrow) without EDTA present in the solution.

Conclusions

We have synthesized a highly versatile disulfide-based snap-top on MSNs and successfully demonstrated the activation of cargo release *via* chemical reduction or photo-excitation either by one UV photon or two near-IR coherent photons. Direct chemical reduction with 2-mercaptoethanol clearly shows that despite the attachment of the bulky 2PNT to the surface of the MSNs, the disulfide still retained its capacity to hold cargo inside the nanopores and release it when the bond is broken. The one-photon experiments prove that the system can be successfully activated with a 408 nm light source that causes electron transfer from 2PNT to the disulfide bond. Finally, we also proved that 2PNT is able to transfer an electron and reduce the disulfide bond with two coherent near-IR photons. To our knowledge, this is the first example of a snap-top disulfide nanovalve activated by two Near-IR photons. The fact that we can use two-photon activation is especially important for use in biological environments owing to higher tissue penetration, greater focal control and the lack of tissue damage with the use of near-IR wavelengths. Mesoporous silica nanoparticles have been shown to be biocompatible but careful tuning and testing would be required for any biological applications. Our system offers a new method for generating photoactivated drug delivery systems that would offer the possibilities of controlled cargo release of a wide variety of drugs.

Acknowledgements

This work was made possible by grants from the NIH RO1 CA133697 and Partner University Fund FACE-PUF 200991853,

and a NIH fellowship to Tania Maria Guardado-Alvarez. MBD gratefully thanks the Conseil Regional d'Aquitaine for financial support (Chaire d'Accueil grant), the Agence Nationale de la Recherche (ANR-2010-NANO-022-01) and the MENSR for a fellowship to Jean-Marie Vabre.

Notes and references

1 K. Furuse, M. Fukuoka, H. Kato, T. Horai, K. Kubota, N. Kodama, Y. Kusunoki, N. Takifuji, T. Okunaka and C. Konaka, *J. Clin. Oncol.*, 1993, **11**, 1852–1857.
2 D. R. Braichotte, G. A. Wagnieres, R. Bays, P. Monnier, V. Bergh and H. E. Den, *Cancer*, 1995, **75**, 2768–2778.
3 D. E. Dolmans, D. Fukumura and R. K. Jain, *Nat. Rev. Cancer*, 2003, **3**, 380–387.
4 J.-O. Yoo and K.-S. Ha, *Int. Rev. Cell Mol. Biol.*, 2012, **295**, 139.
5 D. K. Chatterjee, L. S. Fong and Y. Zhang, *Adv. Drug Delivery Rev.*, 2008, **60**, 1627–1637.
6 Y. N. Konan, R. Gurny and E. Allémann, *J. Photochem. Photobiol., B*, 2002, **66**, 89–106.
7 Y. S. Lin, S. H. Wu, Y. Hung, Y. H. Chou, C. Chang, M. L. Lin, C. P. Tsai and C. Y. Mou, *Chem. Mater.*, 2006, **18**, 5170–5172.
8 M. Liong, J. Lu, M. Kovochich, T. Xia, S. G. Ruehm, A. E. Nel, F. Tamanoi and J. I. Zink, *ACS Nano*, 2008, **2**, 889–896.
9 H. Park, J. Yang, S. Seo, K. Kim, J. Suh, D. Kim, S. Haam and K. H. Yoo, *Small*, 2008, **4**, 192–196.
10 T. M. Guardado-Alvarez, L. Sudha Devi, M. M.-L. Russell, B. J. Schwartz and J. I. Zink, *J. Am. Chem. Soc.*, 2013, **135**, 14000–14003.
11 Q. Lin, Q. Huang, C. Li, C. Bao, Z. Liu, F. Li and L. Zhu, *J. Am. Chem. Soc.*, 2010, **132**, 10645–10647.
12 D. P. Ferris, Y. L. Zhao, N. M. Khashab, H. A. Khatib, J. F. Stoddart and J. I. Zink, *J. Am. Chem. Soc.*, 2009, **131**, 1686–1688.
13 S. Angelos, M. Liong, E. Choi and J. I. Zink, *Chem.–Eng. J.*, 2008, **137**, 4–13.
14 S. Chia, J. Cao, J. F. Stoddart and J. I. Zink, *Angew. Chem.*, 2001, **40**, 2513–2517.
15 C. R. Thomas, D. P. Ferris, J. H. Lee, E. Choi, M. H. Cho, E. S. Kim, J. F. Stoddart, J. S. Shin, J. Cheon and J. I. Zink, *J. Am. Chem. Soc.*, 2010, **132**, 10623–10625.
16 Z. Li, J. C. Barnes, A. Bosoy, J. F. Stoddart and J. I. Zink, *Chem. Soc. Rev.*, 2012, **41**, 2590–2605.
17 M. W. Ambrogio, T. A. Pecorelli, K. Patel, N. M. Khashab, A. Trabolsi, H. A. Khatib, Y. Y. Botros, J. I. Zink and J. F. Stoddart, *Org. Lett.*, 2010, **12**, 3304–3307.
18 M. W. Ambrogio, C. R. Thomas, Y.-L. Zhao, J. I. Zink and J. F. Stoddart, *Acc. Chem. Res.*, 2011, **44**, 903–913.
19 S. Angelos, Y. W. Yang, K. Patel, J. F. Stoddart and J. I. Zink, *Angew. Chem.*, 2008, **120**, 2254–2258.
20 S. Angelos, N. M. Khashab, Y. W. Yang, A. Trabolsi, H. A. Khatib, J. F. Stoddart and J. I. Zink, *J. Am. Chem. Soc.*, 2009, **131**, 12912–12914.
21 R. Casasús, E. Climent, M. D. Marcos, R. Martínez-Máñez, F. Sancenón, J. Soto, P. Amorós, J. Cano and E. Ruiz, *J. Am. Chem. Soc.*, 2008, **130**, 1903–1917.
22 P. DeMuth, M. Hurley, C. Wu, S. Galanie, M. R. Zachariah and P. DeShong, *Microporous Mesoporous Mater.*, 2011, **141**, 128–134.
23 X. Zhang, P. Yang, Y. Dai, P. a. Ma, X. Li, Z. Cheng, Z. Hou, X. Kang, C. Li and J. Lin, *Adv. Funct. Mater.*, 2013, **23**, 4067–4078.
24 Y. Klichko, M. Liong, E. Choi, S. Angelos, A. E. Nel, J. F. Stoddart, F. Tamanoi and J. I. Zink, *J. Am. Chem. Soc.*, 2008, **92**, S2–S10.
25 A. Agostini, F. Sancenón, R. Martínez-Máñez, M. D. Marcos, J. Soto and P. Amorós, *Chem.–Eur. J.*, 2012, **18**, 12218–12221.
26 Y.-L. Zhao, Z. Li, S. Kabehie, Y. Y. Botros, J. F. Stoddart and J. I. Zink, *J. Am. Chem. Soc.*, 2010, **132**, 13016–13025.
27 C. Wang, Z. Li, D. Cao, Y. L. Zhao, J. W. Gaines, O. A. Bozdemir, M. W. Ambrogio, M. Frasconi, Y. Y. Botros and J. I. Zink, *Angew. Chem., Int. Ed.*, 2012, **51**, 5460–5465.
28 K. Patel, S. Angelos, W. R. Dichtel, A. Coskun, Y. W. Yang, J. I. Zink and J. F. Stoddart, *J. Am. Chem. Soc.*, 2008, **130**, 2382–2383.
29 M. You, Z. Zhu, H. Liu, B. Gulbakan, D. Han, R. Wang, K. R. Williams and W. Tan, *ACS Appl. Mater. Interfaces*, 2010, **2**, 3601–3605.
30 T. Takada, C. Tanaka, M. Nakamura and K. Yamana, *Bioorg. Med. Chem. Lett.*, 2010, **20**, 994–996.
31 J. Lu, E. Choi, F. Tamanoi and J. I. Zink, *Small*, 2008, **4**, 421–426.
32 E. Johansson, E. Choi, S. Angelos, M. Liong and J. I. Zink, *J. Sol-Gel Sci. Technol.*, 2008, **46**, 313–322.
33 N. Fomina, C. McFearin, M. Sermsakdi, O. Edigin and A. Almutairi, *J. Am. Chem. Soc.*, 2010, **132**, 9540–9542.
34 S. Kim, T. Y. Ohulchanskyy, H. E. Pudavar, R. K. Pandey and P. N. Prasad, *J. Am. Chem. Soc.*, 2007, **129**, 2669–2675.
35 J. R. Starkey, A. K. Rebane, M. A. Drobizhev, F. Meng, A. Gong, A. Elliott, K. McInnerney and C. W. Spangler, *Clin. Cancer Res.*, 2008, **14**, 6564–6573.
36 M. Pawlicki, H. A. Collins, R. G. Denning and H. L. Anderson, *Angew. Chem., Int. Ed.*, 2009, **48**, 3244–3266.
37 F. Terenziani, C. Katan, E. Badaeva, S. Tretiak and M. Blanchard-Desce, *Adv. Mater.*, 2008, **20**, 4641–4678.
38 M. Blanchard-Desce, *C. R. Phys.*, 2002, **3**, 439–448.
39 W. R. Zipfel, R. M. Williams, R. Christie, A. Y. Nikitin, B. T. Hyman and W. W. Webb, *Proc. Natl. Acad. Sci. U. S. A.*, 2003, **100**, 7075–7080.
40 S. Picard, E. J. Cueto-Diaz, E. Genin, G. Clermont, F. Acher, D. Ogden and M. Blanchard-Desce, *Chem. Commun.*, 2013, **49**, 10805–10807.
41 L. Porrès, V. Alain, L. Thouin, P. Hapiot and M. Blanchard-Desce, *Phys. Chem. Chem. Phys.*, 2003, **5**, 4576–4582.
42 A.-C. Robin, S. Gmouh, O. Mongin, V. Jouikov, M. H. V. Werts, C. Gautier, A. Slama-Schwok and M. Blanchard-Desce, *Chem. Commun.*, 2007, 1334–1336.
43 H. Meng, M. Xue, T. Xia, Z. Ji, D. Y. Tarn, J. I. Zink and A. E. Nel, *ACS Nano*, 2011, **5**, 4131–4144.
44 J. S. Beck, J. C. Vartuli, W. J. Roth, M. E. Leonowicz, C. T. Kresge, K. D. Schmitt, C. T. W. Chu, D. H. Olson and E. W. Sheppard, *J. Am. Chem. Soc.*, 1992, **114**, 10834–10843.

45 C. T. Kresge, M. E. Leonowicz, W. J. Roth, J. C. Vartuli and J. S. Beck, *Nature*, 1992, **359**, 710–712.
46 C. B. Anfinsen and E. Haber, *J. Biol. Chem.*, 1961, **236**, 1361–1363.
47 C. Lu, G. Bucher and W. Sander, *Chem. Phys. Chem.*, 2004, **5**, 399–402.
48 C. Y. Lai, B. G. Trewyn, D. M. Jeftinija, K. Jeftinija, S. Xu, S. Jeftinija and V. S. Y. Lin, *J. Am. Chem. Soc.*, 2003, **125**, 4451–4459.
49 J. L. Vivero-Escoto, I. I. Slowing, C. W. Wu and V. S. Y. Lin, *J. Am. Chem. Soc.*, 2009, **131**, 3462–3463.
50 H. Kim, S. Kim, C. Park, H. Lee, H. J. Park and C. Kim, *Adv. Mater.*, 2010, **22**, 4280–4283.